Precipitation-driven typology of storms in the Alps

Georgia Papacharalampous[1,*], Eleonora Dallan[1], Moshe Armon[2], Joydeb Saha[3], Colin Price[4], Marco Borga[1], and Francesco Marra[5]

[1] Department of Land, Environment, Agriculture and Forestry, University of Padova, Legnaro, Italy

[2] The Fredy and Nadine Herrmann Institute of Earth Sciences, The Hebrew University of Jerusalem, Jerusalem, Israel

[3] National Centre for Medium Range Weather Forecasting, Noida, India

[4] Porter School of the Environment and Earth Sciences, Tel Aviv University, Tel Aviv, Israel

[5] Department of Geosciences, University of Padova, Padova, Italy

[*] Correspondence: georgia.papacharalampous@unipd.it, papacharalampous.georgia@gmail.com

Precipitation-driven typology of storms in the Alps

Georgia Papacharalampous[1,*], Eleonora Dallan[1], Moshe Armon[2], Joydeb Saha[3], Colin Price[4], Marco Borga[1], and Francesco Marra[5]

[1] Department of Land, Environment, Agriculture and Forestry, University of Padova, Legnaro, Italy

[2] The Fredy and Nadine Herrmann Institute of Earth Sciences, The Hebrew University of Jerusalem, Jerusalem, Israel

[3] National Centre for Medium Range Weather Forecasting, Noida, India

[4] Porter School of the Environment and Earth Sciences, Tel Aviv University, Tel Aviv, Israel

[5] Department of Geosciences, University of Padova, Padova, Italy

[*] Correspondence: georgia.papacharalampous@unipd.it, papacharalampous.georgia@gmail.com

Abstract: Numerous advances in precipitation science hinge on our ability to accurately categorize storms into physically meaningful classes, particularly to differentiate between convective and non-convective phenomena. Nonetheless, achieving such classifications remains a challenge for the research community. Here, we propose a precipitation-driven typology of storms in the Alps developed through a straightforward methodology for unsupervised classification. From a vast sub-hourly precipitation dataset, we extracted over 790,000 independent storm time series. To categorize these, we employed a resampling-based partitioning algorithm, optimal in clustering big data. Four storm features (i.e., the maximum intensity, total volume, total duration, and coefficient of variation) drove our typology on an algorithmic basis. The algorithm revealed five dominant storm classes, which we termed as “convective”, “stratiform”, “short stratiform”, “intermittent minor” and “minor” based on a physically-informed examination of their features. Three other features (i.e., the month of the storm initiation, solar time at the first occurrence of the maximum intensity, and lightning count) were used for an independent validation of the classes, together with investigations on the extent to which each class was clustered in space. Consistency with anticipated physical patterns suggests the potential utility of our proposed typology across various modelling applications. These include class-specific stochastic simulation of storms, class-informed bias adjustment of climate model projections or the development of multi-class extreme value analyses. Detailed investigations of its climatological traits revealed, among others, higher convective activity in recent years and specific Alpine regions. We provide the historical occurrences of the proposed storm typology as an open dataset.

Keywords: convective precipitation; storm climatology; storm time series clustering; stratiform precipitation; sub-hourly precipitation; precipitation trends

1. Introduction

Analyzing precipitation storm time series and their climatology is crucial for mitigating hazards such as floods, landslides and debris flows, and adapting to changing climatic conditions (D'Odorico et al. 2005; Merz et al. 2014; Breugem et al. 2020; Kahraman et al. 2021). A specialized branch of such analyses is devoted to the separation of storms into physically meaningful classes, with a particular focus on the differentiation between convective and non-convective events (e.g., Tremblay 2005; Ruiz-Leo et al. 2013; Feloni et al. 2019; Sottile et al. 2021; Dallan et al. 2022; Araujo et al. 2023; Treppiedi et al. 2023; Laaha et al. 2025). Beyond its pivotal role in advancing our comprehension of precipitation processes, this separation has numerous direct implications for stochastic modelling, extreme value analysis, and model uncertainty reduction (Blöschl et al. 2019; Fischer et al. 2019; Fischer and Schumann 2021; Marra et al. 2021; Sottile et al. 2021).

Indeed, the distinct physical mechanisms driving storm generation in each class may necessitate tailored weather generators (e.g., Kaczmarska et al. 2014; Peleg and Morin 2014; Tseng et al. 2025; Laaha et al. 2025) and operational weather forecasting models (e.g., Papadopoulos et al. 2005; Gustafsson et al. 2018; Zhou et al. 2019), or class-specific bias correction methods for climate model simulations (Maraun et al. 2017). At the same time, deriving physically meaningful and, thus, useful storm typologies is challenging, due to the high complexity of the storm generation process, which involves interactions of a variety of physical mechanisms across a wide range of temporal and spatial scales (Grazzini et al. 2019). This challenge is even more difficult, but often necessary, to tackle by using only precipitation data from gauges. For this particular setting, which is also the focus of this study, thresholds on the maximum precipitation intensity or the decorrelation time have been defined to separate storms into types (e.g., Dallan et al. 2022; Araujo et al. 2023). However, these thresholds carry some degree of subjectivity and, consequently, ongoing efforts are devoted to their replacement with more objective methodological means (e.g., Sottile et al. 2021; Treppiedi et al. 2023; Laaha et al. 2025).

Meanwhile, a general storm typology for the entire Alpine range (Section 2.1), a geographically complex territory attracting major interest in the study of precipitation dynamics (e.g., Frei and Schär 1998; Weisse and Bois 2001; Isotta et al. 2014; Ménégoz et al. 2020; Napoli et al. 2023; Estermann et al. 2025) and their links to hydrological extremes (e.g., Blanchet et al. 2025), is still lacking. The closest available storm typology was proposed by Grazzini et al. (2019), which concerns only extreme (heavy) precipitation events in Northern Italy, and requires information on several atmospheric variables, not only precipitation time series, and is not open data that can be used in a variety of modelling contexts, including the class-specific stochastic simulation of storm time series, class-informed bias correction of climate model simulations, and multi-class extreme value methods. Moreover, it was not accompanied by extended analyses of the climatological traits of the storm classes. A particularly urgent need, in this regard, is the detection of trends in the occurrence rates of the various classes (e.g., Rulfová and Kyselý 2014; Llasat et al. 2021; Treppiedi et al. 2023), which may provide direct hints on the expected impacts of the ongoing climate change.

In light of the current gaps in our understanding of the Alpine storm patterns, a clustering analysis relying solely on precipitation measurements from gauges holds significant potential and offers several key advantages. First, it ensures a high degree of applicability across diverse geographical settings. Indeed, supplementary datasets (such as radar or reanalysis) may exhibit limited availability across many locations or may be subject to diverse processing methodologies. Second, it enables a more precise identification of localized rainfall patterns, thereby preventing the misattribution of broad weather system characteristics to specific localized precipitation behaviors. Finally, storm typologies derived from this fundamental data source can provide solid baselines that can be further enriched and contextualized with additional data layers in subsequent analyses.

Given the state-of-the-art and the rationale outlined above, our aims in this study were to:

1) Develop a framework for deriving storm typologies, emphasizing simplicity and versatility, along with objectivity and a demonstrated ability to deliver physically meaningful storm classifications. Simplicity and versatility were also considered important in this context, as they will allow transferability around the globe after marginal adjustments based on the regional climatology or local interests.
2) Introduce an objectively-derived, precipitation-driven typology of Alpine storms. This typology should comprise storm classes with distinct physical meaning and

characteristics, especially those representing convective and stratiform precipitation processes.

3) Investigate the unexplored climatology of the Alpine storm classes by addressing the following key questions:
    a) How does the proportion of the classes vary in space?
    b) How do the occurrence rates of the classes by season vary in space?
    c) Are there temporal changes in the proportion of the classes?

2. Study area and data

2.1 Study area

We studied storms that have occurred in and around the Alps (Figure 1), a region with a wide range of climates — mainly alpine (polar), boreal (snow) and warm temperate, according to the updated Köppen-Geiger classification by Beck et al. (2018). Largely due to the strong influence of mountainous topography on local precipitation especially near the sea (Buzzi et al. 1998), the Alps offer a compelling setting for the study of precipitation storm patterns and their climatology (Rubel et al. 2017). Compared to other regions, the Alps exhibit a higher proportion of high-intensity wet days (Isotta et al. 2014), a larger proneness to extreme storms (Grazzini et al. 2019) and higher lightning counts (Kahraman et al. 2022). The precipitation climatology of the greater Alpine region has been analyzed, for instance, by Frei and Schär (1998), Isotta et al. (2014), Ménégoz et al. (2020) and Napoli et al. (2023). The mean annual precipitation is typically higher than the surrounding floodplains due to orographic enhancement, reaching values as high as 3000 mm year^{-1}. The central region receives lower precipitation amounts, on the order of 900 mm year^{-1}, due to the protection effect played by the surrounding mountains (Borga et al. 2005).

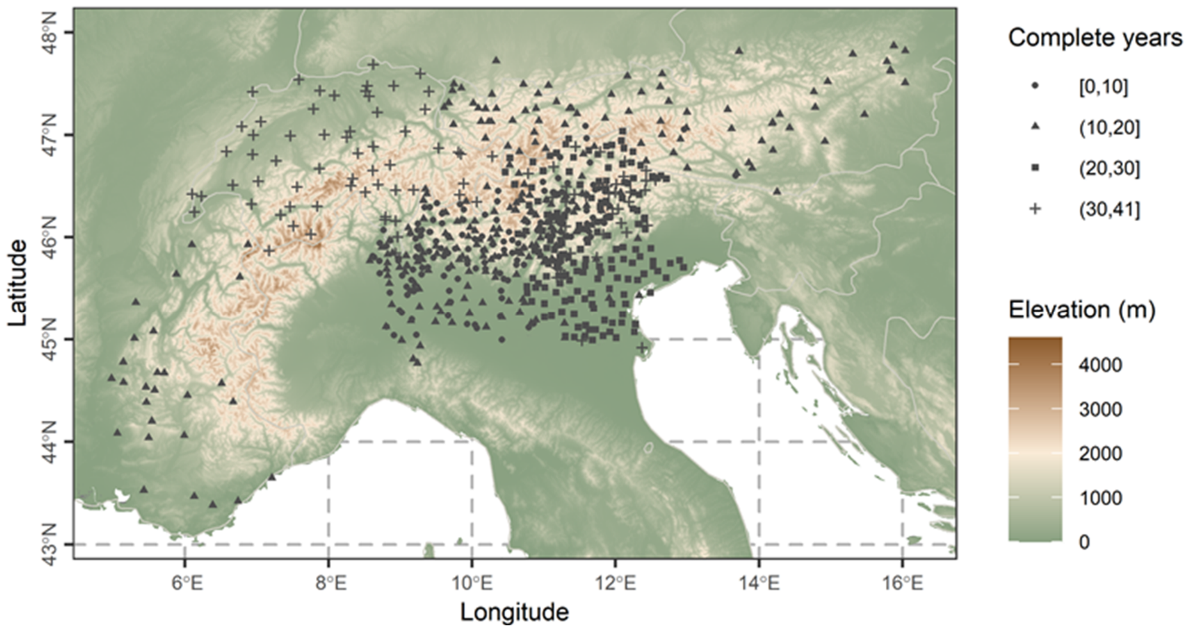

Figure 1. Study area, its topography (extracted from the Amazon Web Services Terrain Tiles), geographical locations of the precipitation stations and number of complete years of available data (from January 1st 00:00:00 to December 31st 23:50:00) for each of these stations.

2.2 Precipitation data

We compiled a comprehensive dataset of sub-hourly precipitation measurements from 670 instrumental stations across five countries (Figure 1): Italy (505 stations), Austria (74), Switzerland (61), France (27), and Germany (3). Based on the Amazon Web Services Terrain Tiles (https://registry.opendata.aws/terrain-tiles), the elevations at the locations of the stations range between –4 and 3,214 m, with a mean and a standard deviation approximately equal to 773 and 627 m, respectively. Subsets of our dataset were previously used in the studies by Dallan et al. (2023, 2024), Marra et al. (2024), Correa-Sánchez et al. (2025) and Peleg et al. (2025), which addressed different research questions. The original data sources are the following:

- Agenzia Regionale per la Prevenzione e Protezione Ambientale del Veneto (https://www.arpa.veneto.it).
- GeoSphere Austria (https://data.hub.geosphere.at/dataset/klima-v1-10min).
- Météo-France (https://meteo.data.gouv.fr).
- MeteoSwiss (https://www.meteoswiss.admin.ch).
- Provincia Autonoma di Trento (https://www.provincia.tn.it).
- Provincia Autonoma di Bolzano (https://meteo.provincia.bz.it/default.asp).

- Agenzia Regionale per la Prevenzione e Protezione Ambientale della Lombardia (https://www.arpalombardia.it).

From these sources, we extracted time series of varying temporal resolutions (5-, 6- and 10-min), which we then homogenized through time series aggregation to the 10- or 12-min temporal resolution, with the latter being the case for the time series from France. Additionally, time zone homogenization was conducted and quality issues (i.e., missing values/dates, negative and other unrealistic values, duplicate dates) were identified and treated. Time series data records corresponding to calendar years with more than 10% of their values missing were excluded from our final dataset. This dataset comprises complete sub-hourly precipitation time series with varying lengths, observed during the course of 44 years (1981–2024). From these time series, we subsequently extracted the precipitation storm time series, as detailed in Section 3.1. The number of complete calendar years per location is summarized in Figure 1. Data for at least 30 complete calendar years are available for 113 locations, allowing for trend analyses (Section 3.5).

2.3 Lightning count data

There is a well-known association between convective precipitation and lightning occurrence (Soriano et al. 2001; Papadopoulos et al. 2005; Pineda et al. 2007). Consequently, lightning counts can be used to independently validate distinctions between convective and non-convective storm time series (Feloni et al. 2019). Such data, and more precisely cloud-to-ground lightning counts derived from the World Wide Lightning Location Network (WWLLN; https://wwlln.net), are available for a large and representative portion of the stations and storms we examined. Herein, we exploited them for the independent validation of the precipitation storm classes (Section 3.4). Detailed information about the WWLLN network can be found in Rodger et al. (2006) and Virts et al. (2013). Given that the storms often spanned multiple days, the maximum daily lightning count was extracted for each storm. To ensure consistency and account for uncertainty in the geolocation, lightning strikes were counted within a ±0.5° grid box centered on the location of each station. Temporal alignment was achieved by matching the WWLLN lightning data to the storm time ranges.

3. Methods

3.1 Storm time series extraction

Precipitation storm time series, representing wet periods that are independent in time, were extracted from the merged precipitation dataset (Section 2.2) following the methodology described in Marra et al. (2020). Considering the climatology of the Alps, independence was ensured by imposing the lower threshold of 24 hours in the length of the dry spells between storms. Storms with duration of at least 30 min were included in our precipitation storm database.

3.2 Storm clustering

To classify the precipitation storm time series, we formulated a methodology employing unsupervised machine learning (Hastie et al. 2009, ch. 14; James et al. 2013, ch. 10). This approach is increasingly used for developing storm typologies (e.g., Grazzini et al. 2019; Sottile et al. 2021) and, more generally, event typologies in the field of hydrology (e.g., Markonis et al. 2021; Fischer and Schumann 2024), owing to its objectivity and scalability—qualities that align well with the objectives of this study. Our clustering methodology is feature-based, aiming at maximizing intra-cluster homogeneity and inter-cluster heterogeneity based on the following four diverse features extracted from the precipitation storm time series (Section 3.1): (a) maximum (peak) intensity, (b) total volume, (c) total duration, and (d) coefficient of variation. The first three, in particular, are established as key features in the study of storms (e.g., Herrera et al. 2023), while the coefficient of variation is a standard feature in stochastic analysis that can also be used to quantify gradients of variability. To maintain simplicity and avoid redundancy, we did not employ more features for the clustering.

To address scalability challenges (specifically, the large RAM storage requirements) posed by our large dataset (Section 2.2), which could not be handled by conventional non-hierarchical clustering algorithms (e.g., the well-known k-means and k-medoids described in detail in Hastie et al. 2009, ch. 14.3.6 and 14.3.10), we selected CLARA (Clustering Large Applications; Kaufman and Rousseeuw 1990, ch. 3) as the core algorithm. In summary, CLARA is a resampling-based partitioning algorithm (Hopke and Kaufman 1990) applying k-medoids. These exhibit larger robustness to noise and outliers with respect to k-means, as they use actual data points (the "medoids") as cluster centers instead of computing their cluster centers (the "centroids"). Within CLARA's framework, the k-medoids are applied to cluster a random sample of the data, with this process being repeated multiple times. The best clustering solution is then selected based on a minimum dissimilarity distance measure and finally applied to the entire dataset. In this study, the sample number and sample size were set to 10,000 and 1,000, respectively. The dissimilarities were calculated using euclidean distances.

To ensure that CLARA would not be affected by skewness and different scales in the features, feature preprocessing took place. More precisely, the feature values were first transformed and then standardized. Log-transformation was applied to the maximum intensity, total volume and total duration, and square-root transformation was applied to the coefficient of variation (due to the existence of zeros in the values of this latter feature). Standardization of the storm duration and coefficient of variation took place for all the stations together, while it was done for each station separately, for the maximum intensity and total volume. This distinction was made because the latter two features are expected to strongly depend on local climatological conditions, in contrast to the former two (e.g., Avanzi et al. 2015).

3.3 Storm type validation

The storm classes, obtained through clustering, were initially explored using the four defining features (Section 3.2) alongside visually inspecting the precipitation storm time series. Names were assigned to each class on its characteristics and expert knowledge. An independent physical validation was then conducted to ensure robustness and generalizability of the clustering outcome. The first phase of this validation relied on three features that were not involved in the clustering: seasonality (month at the storm initiation), diurnal cycle (solar time at the first occurrence of the maximum intensity — note that the maximum intensity may appear more than once in storm time series, especially for sub-hourly temporal resolutions) and lightning count. The month at the storm initiation was extracted from the storm time series (Section 3.1). The solar time at the (first) occurrence of the maximum intensity was chosen over the local time to better reflect the sun's position in the sky and its influence on storm dynamics. It was estimated based on the respective UTC time (which was extracted from the storm time series; Section 3.1) and the longitude at the location of the storm. Lightning count validation was performed on a reduced but still large sample, due to limitations in the availability of lightning data (Section 2.3).

The second phase of the independent validation employed spatial clustering tests. In fact, to make sure they have a physical meaning, it is important that the clusters identified from local time series have a spatial consistency. For those, we computed the occurrence rate of each storm class in the neighborhood of each given class on the same day. To do so, we examined each storm in each station, inspecting distance intervals (km) from occurrences of the storm itself and other storm classes in distance intervals of: (0, 10], (10, 20], (20, 50], (50, 100], (100, 200], and (200, 500] km. We only included storms in this computation, meaning that dry stations in the examined neighborhood were not considered.

Additionally, we examined the spatial pattern of storm states across the Alpine range for eight case studies. These included random dates in the winter and early spring (2006-03-10, 2012-01-08, 2013-01-27), as well as dates when events that are well-known to the research community occurred in the region of interest, such as the Vaia storm (2018-10-29; Davolio et al. 2020), the Lausanne flood (2018-06-11; Gabella et al. 2019), the Vizze flood (2012-08-04; Destro et al. 2018), the Magra flood (2011-10-25; Amponsah et al. 2016), and the Lierza flood (2014-08-02; Borga et al. 2019).

3.4 Storm type climatology analysis

We performed a climatology analysis of the storm classes. The analysis included three independent parts. In the first, we computed the occurrence rates of each class at each geographical location. In the second, we computed seasonal (DJF, MAM, JJA, SON) occurrences within each class at each geographical location. To make the identification of spatial patterns easier, the occurrence rates (%) from the first two parts were grouped into the following categories: [0, 10], (10, 20], (20, 30], (30, 40], (40, 50], (50, 60], (60, 70], (70, 80], (80, 90], and (90, 100]. The last part of the analysis focuses on the climatology variations in time, and was conducted in two steps: (a) Computation of the occurrence rates of the classes within each of the consecutive time periods 1981-1990, 1991-2000, 2001-2010, and 2011-2023; and (b) Trend analysis for 113 stations with at least 30 complete years of precipitation data (Figure 1). The latter comprised the computation of the slope of the linear regression line and performance of the Man-Kendall trend test (Mann 1945; Kendall 1975), with the null hypothesis being correlation zero (no monotonic trend) and p-values smaller or equal to 0.05 suggesting strong evidence against the null hypothesis and, thus, trend. Both (a) and (b) were conducted for three different settings: all seasons combined; summer only (JJA); and the remaining seasons (DJF, MAM and SON).

4. Results and discussion

4.1 Precipitation storm database

Our precipitation dataset yielded a collection of 792,786 storm time series of varying sizes and characteristics (Appendix A). The size of this collection surpasses that of the largest existing precipitation storm collections (e.g., Herrera et al. 2023), as well as that of other remarkably large event datasets in the field (e.g., Stein et al. 2020; Tarasova et al. 2020). Combined with its fine (sub-hourly) temporal resolution, this dataset provides a robust basis for our storm typology.

4.2 Analyzing storm types through their driving features

The division into five classes led to physically interpretable results in terms of the features driving the clustering (Figure 2), consistent with our aim to derive a storm typology that satisfactorily reflects precipitation in the Alps. The key role of this knowledge in validating clusters towards achieving optimal clustering solutions is emphasized in the statistical learning literature (James et al. 2013, ch. 10.3). Indeed, divisions into fewer classes did not allow classes representing convective and stratiform phenomena to discernibly emerge, while divisions into more classes led to outcomes without anticipated physical meaning. For instance, a six-cluster division yielded a similar structure, with one of our five clusters being subdivided into two without a clear physical justification.

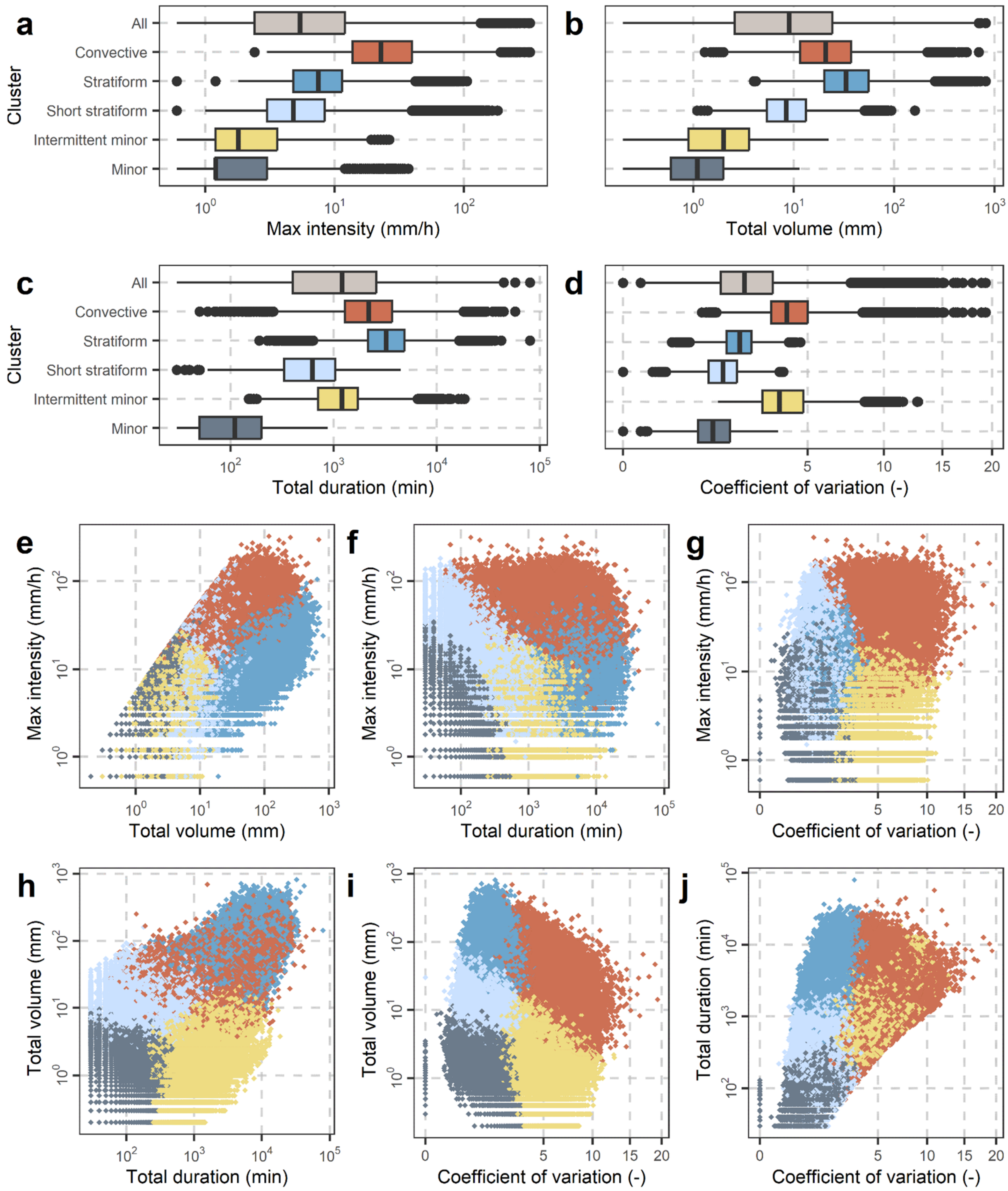

Figure 2. Analysis of the (a) maximum intensity, (b) total volume, (c) total duration and (d) coefficient of variation values characterizing the clusters, and (e-j) investigations of the relationships between these values.

Overall, a five-class typology seems reasonable. We expected at least two important classes to emerge—one related to convective processes and another related to stratiform processes. Additionally, one or more classes would include observations of less significant phenomena or events that our gauge-based time series cannot fully capture, due to the fine time resolution and limited spatial coverage of the rain gauges. These expectations are in alignment with previous storm classification studies, such as Rulfová and Kyselỳ (2013) and Cipolla et al. (2020), which include classes comprising the "mixed" and "unresolved" events, or Sottile et al. (2022), who clustered 10-min precipitation storm time series observed in Sicily, Italy into four categories (two of convective nature, one of possibly convective nature and one of stratiform nature). The same expectations are also reasonable in light of Grazzini et al. (2020), who considered three classes (of frontal, intermediate and deep convective origins) while classifying only the extreme storm events in the Alps.

We named the classes as "convective" (156,295 storms), "stratiform" (182,309 storms), "short stratiform" (190,385 storms), "intermittent minor" (136,056 storms) and "minor" (127,741 storms), based on the physical examination of their driving features (Figure 2). Indeed, the "convective" class comprises the storms with the highest maximum intensities (Figure 2a), among the highest total volumes (Figure 2b) and the highest coefficient of variation values (Figure 2d). Moreover, the "stratiform" storms exhibit features typically attributed to stratiform storms and, more precisely, medium maximum intensities (Figure 2a), the highest total volumes (Figure 2b), the longest total durations (Figure 2c) and low coefficient of variation values (Figure 2d). The "short stratiform" class is characterized by maximum intensities and coefficients of variation of similar magnitude as the stratiform class (Figure 2a, d), though its total volumes are somewhat smaller (Figure 2b) and its total duration is much shorter (Figure 2c). Thus, we hypothesize it represents stratiform events where winds are orthogonal to the main cloud direction, resulting in similar properties to typical stratiform storms, but with a shorter total duration. Lastly, the "intermittent minor" and "minor" classes have mostly low maximum intensities (Figure 2a) and mostly low total volumes (Figure 2b). The latter contains all the minor storms with short total durations and low coefficient of variations, and the "intermittent minor" those with medium total durations and high coefficient of variations (Figure 2c, d). Visual examination reveals that the "intermittent minor" class comprises storm time series resembling those of the "minor" class but punctuated by relatively long dry periods. The "intermittent minor" and "minor" classes likely reflect intermittent station exposure to storm events, a fact highlighting the challenges in establishing a fully definitive and physically consistent typology from point measurements.

More generally, when interpreting the derived storm types, it is essential to consider the nature of our clustering approach, which was station-based (or time series-based).

For instance, the long total duration and relatively high occurrence rate (approximately 20%) of the "convective" class, which might initially appear inconsistent with typical characteristics of convective processes, are better interpreted considering the methodological context, in which the entire storm is classified and not only its convective component. Moreover, our storm classes demonstrate robustness to data perturbations. Indeed, subsampling experiments that included the removal of entire regions (results not presented here for reasons of brevity) consistently produced classes with similar features. This robustness is a notable advantage, as many clustering methods are sensitive to such perturbations (James et al. 2013, ch. 10.3.3).

Furthermore, in their review of flood classifications, which offers insights that are also applicable to storm classifications, Tarasova et al. (2019) identify robustness (which they define as the ability to obtain similar classes using different data sources) as a critical characteristic for event typologies. In addition, while the exact form of our storm types may not be globally transferable, our clustering methodology is, due to its simplicity and versatility. Consequently, our overall framework also aligns with the transferability and adaptability requirements emphasized in the same review.

4.3 Validating storm types through independent features

The successful separation of the "convective" class from the remaining storm classes was further confirmed by our analysis of independent features (i.e., features that were not used for developing the typology) of the classes. Convective precipitation phenomena are indeed known to appear more often during and around summer in the Alps (Figure 3a), to be more common when the sun has warmed the ground enough leading to air lifting movements (Figure 3b), and to be accompanied by notable lightning activity (Figure 3c). As stratiform phenomena are more common in spring and autumn in the Alps, the seasonal analysis also validates the successful separation of the "stratiform" class from the rest (Figure 3a), showing a bimodal distribution for those storms.

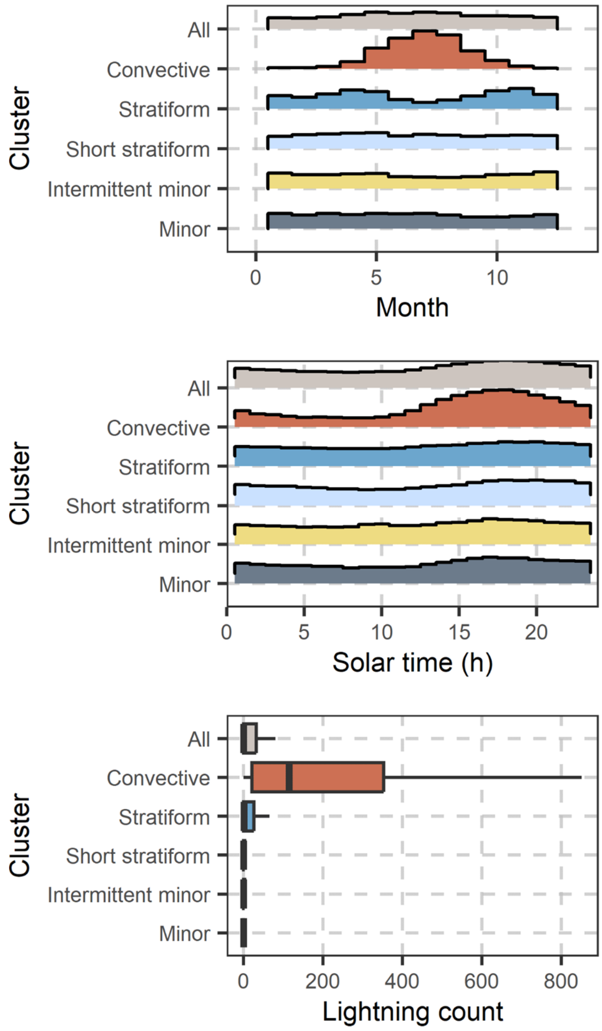

Figure 3. Analysis of the clusters with respect to their: (a) seasonality, (b) solar time at the (first) occurrence of the maximum intensity and (c) lightning counts (outliers have been removed for clarity).

4.4 Validating storm types through spatial organisation investigations

Spatial organisation is found to characterize the historical occurrences of all the storm classes, with each of them having occurred far more commonly around itself during the same day than any other class, at least for distances up to 50 km (Figure 4; see the side-by-side boxplots on the main diagonal thereon). As one would expect, the "stratiform" class is characterized by the largest degree of spatial clustering. Its historical occurrence rates exhibit a median equal to about 75% for distances smaller than 10 km far from itself. This means that storms observed within 10 km from storms classified as "stratiform", are classified with the same type about 75% of the time. This median reduces gradually to about 50% for distances of 200 to 500 km away from the analyzed storm. With the respective occurrence rates being found equal to about 65% (55%) and larger than 30%

(15%), the "convective" class ("short stratiform" class) is characterized by the second (third) largest degree of spatial clustering and graduality in the reduction of these rates with the distance. The large degree of spatial clustering observed for the "convective" class, though seemingly inconsistent with typical intuitions about convective precipitation, becomes understandable considering the nature of our clustering problem; our method classifies the entire storm time series, not solely the moments of convection appearing in those. Additionally, while individual convective cells are in fact localized, they are then advected and can cover a relatively large area over the time of the storm.

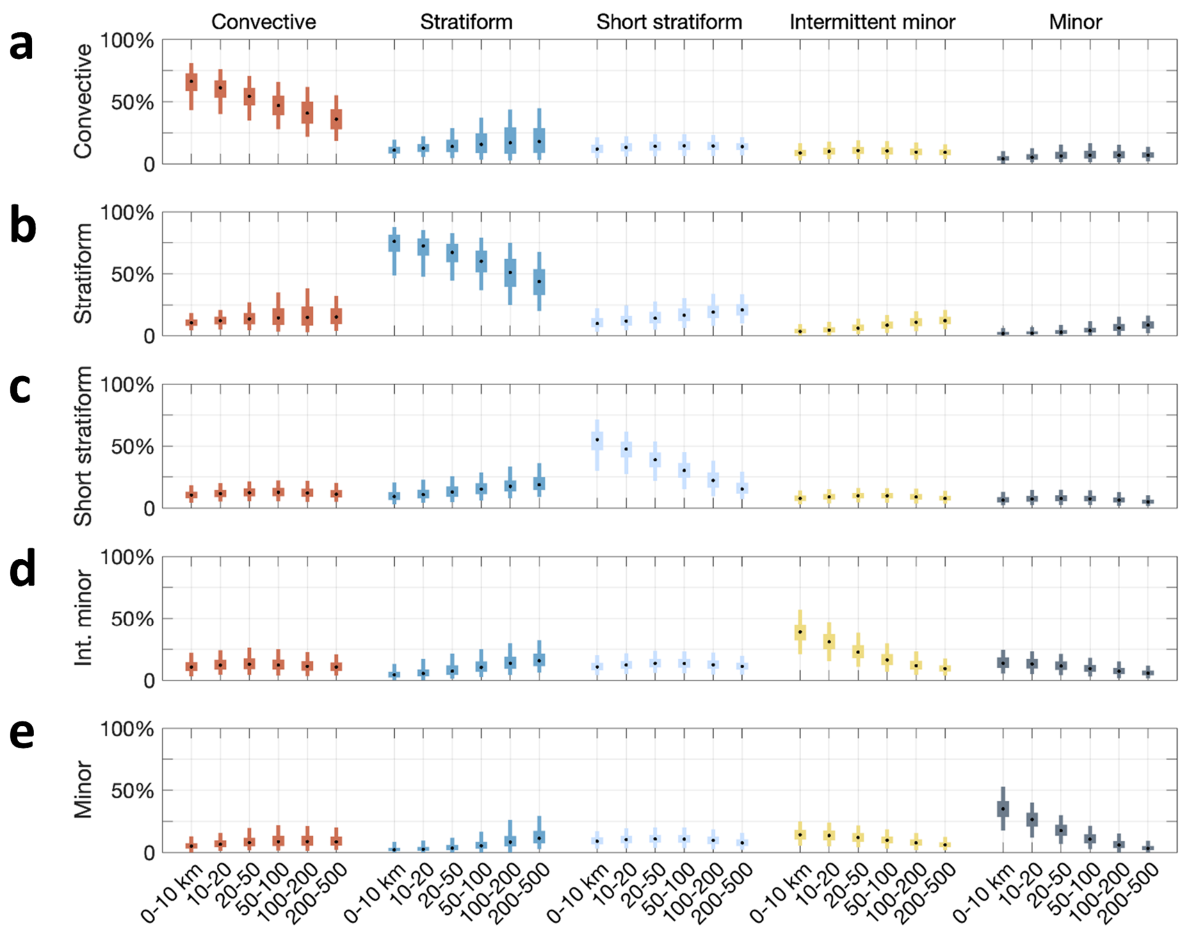

Figure 4. Occurrence rates of the classes in the wet stations within various ranges of distances from the (a) "convective", (b) "stratiform", (c) "short stratiform", (d) "intermittent minor" and (e) "minor" classes.

For the "intermittent minor" and "minor" classes, the reduction in the occurrence rates around themselves is more abrupt. This is in accordance with our expectations, as these classes are expected to be linked to unimportant storms or phenomena that were not well-captured by our gauges. For example, we expect the stations that only capture the outermost portions of an important event to only see a minor amount of precipitation.

Indeed, the median of these rates starts from about 40% for distances less than 10 km and becomes less than 25% already for distances between 20 and 50 km. Moreover, as the distance from a storm observation increases, the occurrence rates of different classes increase notably for some pairs of classes, such as the {“stratiform”, “convective”}, {“stratiform”, “short stratiform”}, {“stratiform”, “intermittent minor”} and {“stratiform”, “minor”}. For other pairs, such as {“intermittent minor”, “minor”} and {“short stratiform”, “convective”}, they remain similar or tend to only slightly increase.

Figure 5 offers a more intuitive understanding of the historical occurrence rates, as well as case-specific insights contributing to the overall validation. In the winter and early spring (Figure 5a, c, e), the “stratiform”, “short stratiform”, “intermittent minor” and “minor” storm classes display noticeable spatial clustering, with this clustering being more intense for the former two classes. On the contrary, “convective” storm occurrences were randomly distributed during these seasons, lacking any apparent spatial clustering. However, on dates with high-impact storm events (Figure 5b, d, f-h), the “convective” storms also displayed strong spatial clustering, with the “convective” phenomena having occurred in quite large areas in many cases. In contrast, the “intermittent minor” and “minor” storm occurrences were few and randomly distributed on these dates, typically on the edge of the wet region.

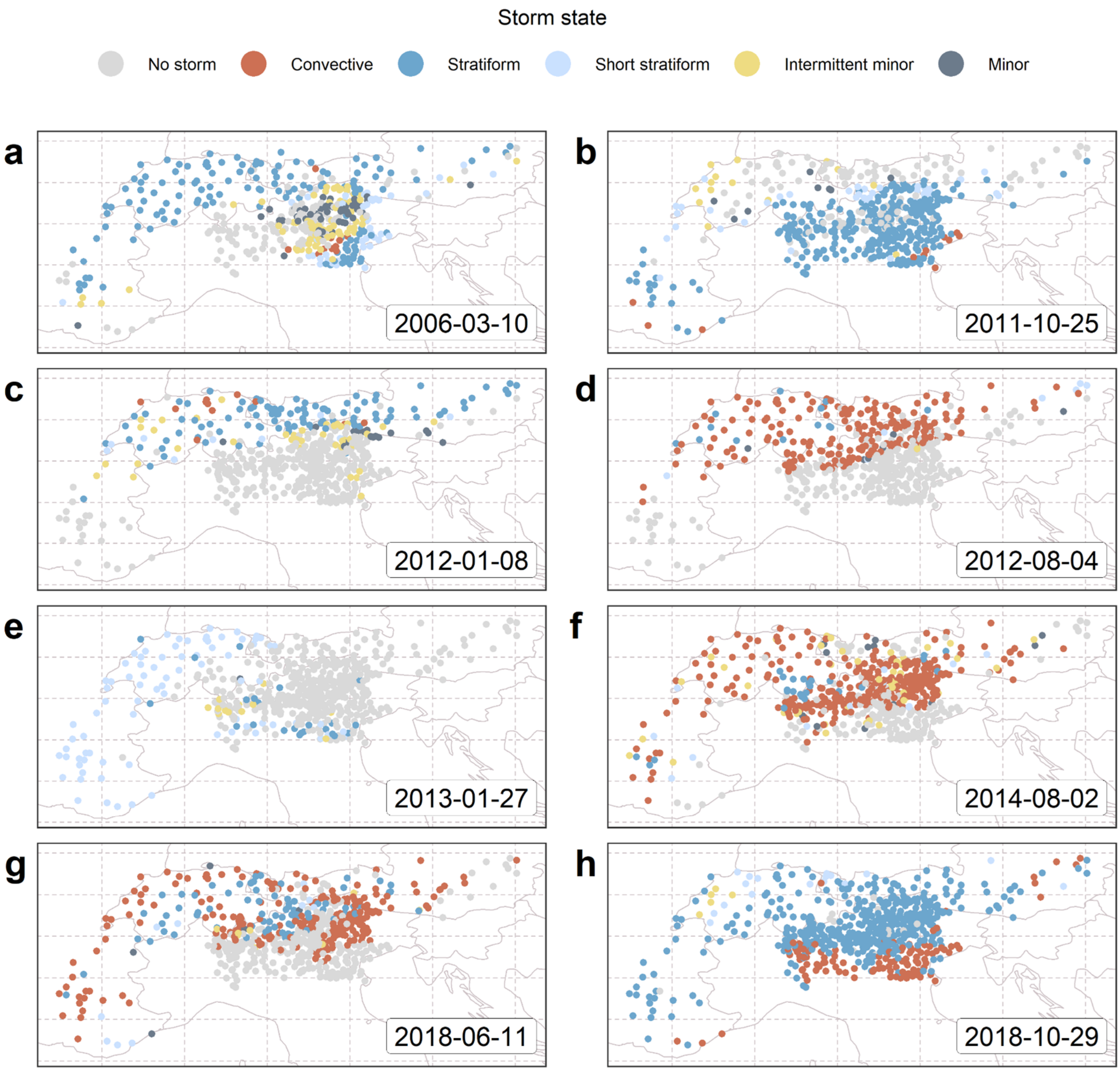

Figure 5. Storm state at stations with data on (a, c, e) random dates in the winter or early spring and (b, d, f-h) dates when well-known storm events occurred.

Notably, heavy rainstorms with large spatial extent were observed in northern Italy on October 25, 2011 (Amponsah et al. 2016), which our clustering method attributed to "stratiform" phenomena (Figure 5b). Also notably, the storm that led to a severe flash flood and numerous debris flows in the Vizze valley (Eastern Italian Alps) on August 4, 2012, (Marra et al. 2014; Destro et al. 2018) was classified as "convective" (Figure 5d). On August 2, 2014 (Figure 5f), high-intensity, short-duration rainfall caused the Lierza river (Eastern Italian prealps) to burst its banks, leading to severe flash flooding and landslides in Veneto, northern Italy (Borga et al. 2019). Our clustering method identified "convective" storms in those areas on that date. Similarly, on the late evening of June 11, 2018 (Figure 5g), heavy thunderstorms and a record-breaking, high-intensity, short-duration storm caused flash flooding in Lausanne, Switzerland (Gabella et al. 2019). Our clustering method accurately classified the storm occurrences near Lausanne on this date as "convective". Finally, the Vaia storm that severely hit north-eastern Italy at the end of October, 2018 (Davolio et al. 2020), was identified, consistent with Davolio et al. (2020), as "stratiform" with vast regions of "convective" features mostly in the southern lowlands (Figure 5h).

4.5 Storm type climatology

Figure 6 illustrates the historical proportions of the classes across the examined locations. Overall, "convective" storms (Figure 6a) occurred at rates between 10% and 20% in many locations, including those in Switzerland and Germany, most of those in France and Austria, and about half of those in Italy. In the remaining locations, mostly including the largest part of Northeastern Italy, "convective" storm occurrence ranged from 20% and 30%. The "stratiform" storms (Figure 6b) were prevalent, occurring at rates from 20% to 30% in most Italian areas and some locations in France, Switzerland, Germany, and Austria. Only a few lowland locations in Italy showed lower occurrences of this storm type. Higher occurrences, between 30% and 40%, were observed at the remaining locations. Rates of the "short stratiform" storms (Figure 6c) were more consistent across the various locations, with most experiencing occurrences between 20% and 30%. Small variations existed, with a few locations exhibiting rates slightly outside this range, either 10% to 20% or 30% to 40%. Lastly, each of the minor classes (Figure 6d, e) generally represented 10% to 20% of the occurrences for most locations. However, the "intermittent minor" storms (Figure 6d) were more frequent for most of the examined lowland locations in Italy, reaching occurrence rates between 20% and 30%.

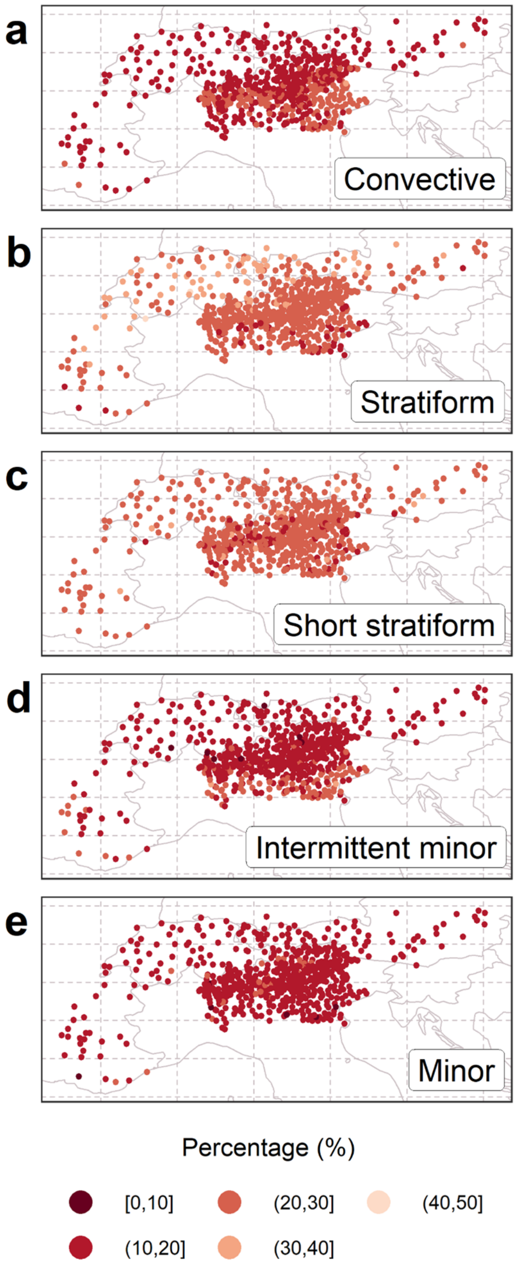

Figure 6. Proportions of the (a) “convective”, (b) “stratiform”, (c) “short stratiform”, (d) ”intermittent minor” and (e) “minor” classes in each geographical location.

Distinct spatial patterns characterize the historical occurrence rates of the "convective" (Figure 7a, d, g, j) and "stratiform" (Figure 7b, e, h, k) storm classes across the four seasons. For nearly all locations, the "convective" class occurs at very low rates during winter (DJF), as confirmed by Figure 3a, resulting in no notable spatial patterns for that season (Figure 7a). In contrast, "convective" storms are most frequent in summer (JJA), and their occurrence rates (Figure 7g) reveal clear meteorological differences across regions. Specifically, "convective" storms become more common moving from south to north and from lowlands to highlands. This pattern likely reflects the role of Alpine topography in triggering convective lifting through orographic effects. In the spring (MAM) and autumn (SON), "convective" storms appeared more often in low locations in Italy than in the pre-Alps and Alps, experiencing occurrences, in most cases, between 20% and 30% and between 10% and 20%, respectively. In the same seasons, the "stratiform" storms showed occurrence rates that do not reveal clear spatial patterns. In the winter, they mostly occurred with lower rates for the pre-Alpine and Alpine areas in Italy than for other regions, while in the summer they occurred with low rates for the low elevation locations in Italy and for the south locations in France and with somewhat larger rates for the remaining regions. On the other hand, no notable spatial patterns were observed for the occurrence rates in the four seasons of the "short stratiform" storms (Figure 7c, f, i, l).

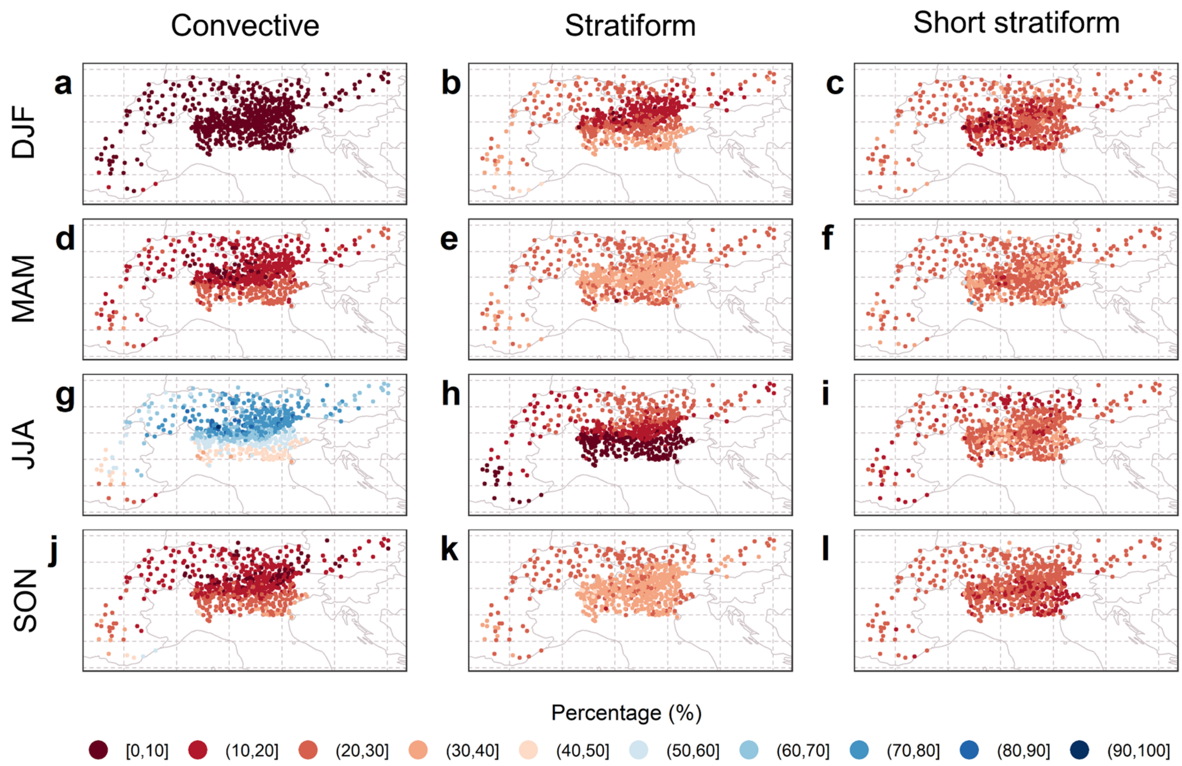

Figure 7. Proportions of the seasons within the (a, d, g, j) "convective", (b, e, h, k) "stratiform" and (c, f, i, l) "short stratiform" classes.

Notable positive temporal changes were identified in the occurrence rates of the "convective" class, thereby reinforcing the findings by Dallan et al. (2022), that reported an increasing trend in extreme short-duration precipitation in the north-eastern Italian Alps and associated it to enhanced convective activity in the summer. Our results suggest that this signal is not limited to the area analysed by these authors but pertains to the entire Alpine area. Recent findings by Dallan et al. (2024) and Estermann et al. (2025) reported that this increasing trend in extreme (heavy) precipitation in northeastern Italy and the greater Alpine region is expected to continue in the future, based on analyses of climate model projections. Although noteworthy changes were observed across all seasons (Figure 8a, d), the summer changes (Figure 8b, e) were far more prevalent than those in the other seasons (Figure 8c, f). In particular, the trends were found to be statistically significant for about 22% and 27% of the stations offering long records for all the seasons (Figure 8d) and for summer (Figure 8e), respectively. At the same time, notable negative temporal changes were found for the occurrence rates of the "stratiform" and "short stratiform" classes, especially for the summer season (Figure 8b, e), with the respective percentages of the stations with statistically significant trends being found equal to about 16% for the "stratiform" and 19.5% for the "short stratiform".

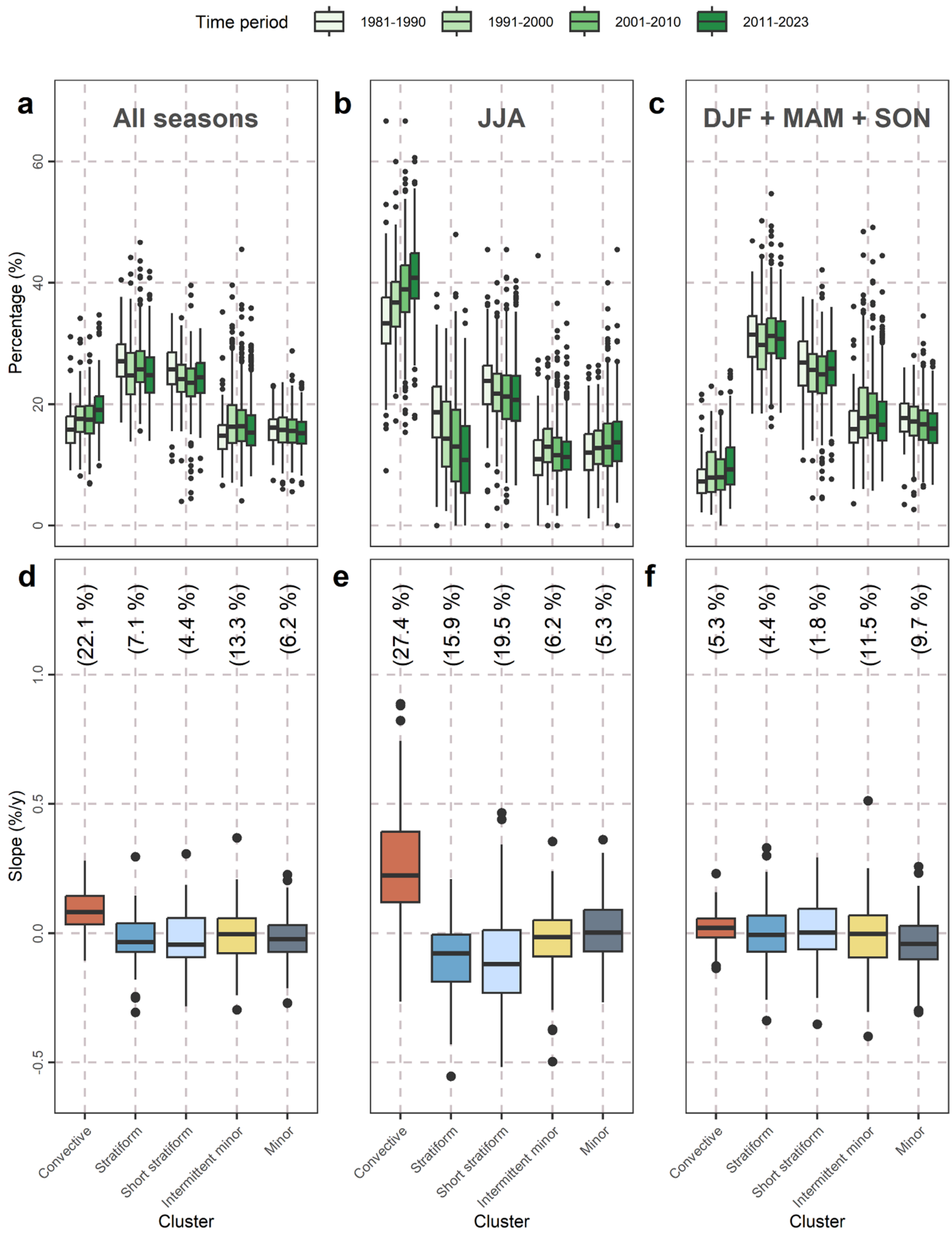

Figure 8. Analyses of the temporal changes in the proportion of the clusters at the various stations: (a-c) Percentages of the clusters within consecutive time periods, and (d-f) trend analyses for the 113 stations offering at least 30 complete years of precipitation data (see Figure 1), with the percentages of the stations with statistically significant trends being reported at the top of the side-by-side boxplots of the linear slope estimates.

5. Summary and conclusions

This study introduces a precipitation-driven typology that separates the Alpine storms into five classes. This typology was informed by a collection of over 790,000 sub-hourly time series of independent storms extracted from a vast precipitation dataset spanning the Alpine range across five countries. A clustering method played a central role in the development of our proposed typology. This method objectively draws information from four key storm features estimated using precipitation time series: (a) maximum intensity, (b) total volume, (c) total duration, and (d) coefficient of variation. It was designed for simplicity and versatility to enable adaptations to diverse regions around the globe through marginal adjustments reflecting region-specific climatological characteristics. In particular for the Alpine region, the robustness of the clustering method in its current configuration was confirmed through its application to subsets of our storm collection. Because of its known optimality in clustering big data, a resampling-based partitioning algorithm was employed herein. Nonetheless, conventional partition-based clustering algorithms, such as the k-means or k-medoids, are expected to exhibit similar efficiency in the absence of scalability issues.

Three additional storm features not used for the clustering, specifically the month of the storm initiation, solar time at the (first) occurrence of the maximum intensity and lightning count corresponding to the storm, were used in this study for the physical validation of the derived classes, along with an examination of the extent to which the occurrences of each class were clustered in space. Overall, the validation showed consistency with anticipated physical patterns, especially regarding the distinction of crucial significance between the convective and non-convective phenomena, and guided the naming of the classes as “convective”, “stratiform”, “short stratiform”, “intermittent minor” and “minor”.

Fundamental questions in the study of storm typologies concern the climatology of the classes. For the Alps, we found the occurrence rates of the “convective” storms to depend both on the location and the season, and identified regions where the same rates were higher than in others for specific seasons, such as the lower-elevation regions in Italy during spring. We also found the “convective” storms to be occurring with increasing frequency in more recent years, particularly during summertime. These findings underscore the utility of our proposed typology for understanding the complex dynamics of Alpine precipitation and reinforce our belief that this typology offers a robust framework for a variety of modelling purposes in the Alps.

Based on the physical consistency observed, we deem that the proposed typology can meet various direct methodological uses within the Alpine region, extending beyond the climatological analysis application conducted in this study. These could range from the development of stochastic simulation methods tailored to the characteristics of the storms to the improvement of the bias correction of our climate model projections or to the development of process-based extreme value analyses. Thus, we provide the historical occurrences of the classes, together with the storm features, in the form of an open dataset (Appendix A).

Declaration of competing interest: There is no conflict of interest.

Acknowledgements: This study was carried out within the RETURN Extended Partnership and received funding from the European Union Next-GenerationEU (National Recovery and Resilience Plan – NRRP, Mission 4, Component 2, Investment 1.3 – D.D. 1243 2/8/2022, PE0000005). The work and the data collection were supported by the INTENSE project (raINfall exTremEs and their impacts: from the local to the National ScalE) funded by the European Union - Next Generation EU in the framework of PRIN (Progetti di ricerca di Rilevante Interesse Nazionale) programme (grant 2022ZC2522) and by the "The Geosciences for Sustainable Development" project (Budget Ministero dell'Università e della Ricerca–Dipartimenti di Eccellenza 2023–2027 C93C23002690001). MA was supported by the energy and climate science grant for faculty by The Council for Higher Education in Israel. We thank Marika Koukoula, Nadav Peleg, Dario Treppiedi, Assumpta Ezeaba and Arturo Cesar Sanchez-Peña for handling parts of the rain gauge data.

Appendix A Data availability and statistical software

Information about the 792,786 precipitation storm time series extracted and analyzed in this study is provided in the form of an open dataset (Papacharalampous et al. 2025). This information is the following: the geographical location where each storm was observed indicated by its longitude and latitude, the timestamps at the storm initiation and termination, the storm features that drove the proposed typology on an algorithmic basis (i.e., maximum intensity, total volume, total duration, and coefficient of variation) and the storm type. The original time series cannot be shared by the authors; the sources of the original precipitation data are cited in the article (Section 2).

Data processing relied on a combination of the `MATLAB` and `R` (R Core Team 2024) programming languages. The statistical analyses and visualizations were conducted in `R`, with the exception of the computational analyses on spatial clustering, including the creation of Figure 4, which were performed in `MATLAB`. The following `R` packages were utilized: `bdc` (Ribeiro et al. 2024), `cluster` (Maechler et al. 2023), `data.table` (Barrett et al. 2024), `devtools` (Wickham et al. 2022), `dplyr` (Wickham et al. 2023a), `elevatr` (Hollister 2023), `ggpubr` (Kassambara 2023), `ggridges` (Wilke 2024), `gplots` (Warnes et al. 2024), `knitr` (Xie 2014, 2015, 2024), `lubridate` (Grolemund and Wickham 2011, Spinu et al. 2024), `raster` (Hijmans 2025), `RColorBrewer` (Neuwirth 2022), `readxl` (Wickham and Bryan 2023), `rmarkdown` (Allaire et al. 2024, Xie et al. 2018, 2020), `rnaturalearth` (Massicotte and South 2023), `scales` (Wickham et al. 2023b), `streamMetabolizer` (Appling et al. 2018) and `tidyverse` (Wickham et al. 2019, Wickham 2023).

References

[1] Allaire JJ, Xie Y, Dervieux C, McPherson J, Luraschi J, Ushey K, Atkins A, Wickham H, Cheng J, Chang W, Iannone R (2024) rmarkdown: Dynamic Documents for R. R package version 2.29. https://CRAN.R-project.org/package=rmarkdown.

[2] Amponsah W, Marchi L, Zoccatelli D, Boni G, Cavalli M, Comiti F, Crema S, Lucía A, Marra F, Borga M (2016) Hydrometeorological characterisation of a flash flood associated with major geomorphic effects: Assessment of peak discharge uncertainties and analysis of the runoff response, Journal of Hydrometeorology 17:3063–3077. https://doi.org/10.1175/JHM-D-16-0081.1.

[3] Appling AP, Hall Jr RO, Yackulic CB, Arroita M (2018) Overcoming equifinality: Leveraging long time series for stream metabolism estimation. Journal of Geophysical Research: Biogeosciences 123(2):624–645. https://doi.org/10.1002/2017JG004140.

[4] Araujo DS, Marra F, Ali H, Fowler HJ, Nikolopoulos EI (2023) Relation between storm characteristics and extreme precipitation statistics over CONUS. Advances in Water Resources 178:104497. https://doi.org/10.1016/j.advwatres.2023.104497.

[5] Avanzi F, De Michele C, Gabriele S, Ghezzi A, Rosso R (2015) Orographic signature on extreme precipitation of short durations. Journal of Hydrometeorology 16:278–294. https://doi.org/10.1175/JHM-D-14-0063.1.

[6] Barrett T, Dowle M, Srinivasan A, Gorecki J, Chirico M, Hocking T, Schwendinger B (2024) data.table: Extension of 'data.frame'. R package version 1.16.4. https://CRAN.R-project.org/package=data.table.

[7] Beck HE, Zimmermann NE, McVicar TR, Vergopolan N, Berg A, Wood EF (2018) Present and future Köppen-Geiger climate classification maps at 1-km resolution. Scientific Data, 5(1):1–12. https://doi.org/10.1038/s41597-023-02549-6.

[8] Blanchet J, Reverdy A, Blanc A, Creutin JD, Kiennemann P, Evin G (2025) Linking torrential flood event occurrence to weather-type conditional driving atmospheric conditions—The case of the Northern French Alps. Journal of Hydrology: Regional Studies 59:102402. https://doi.org/10.1016/j.ejrh.2025.102402.

[9] Blöschl G, Bierkens MFP, Chambel A, Cudennec C, Destouni G, Fiori A, Kirchner JW, McDonnell JJ, Savenije HHG, Sivapalan M, et al. (2019) Twenty-three Unsolved Problems in Hydrology (UPH) – A community perspective. Hydrological Sciences Journal 64(1):1141–1158. https://doi.org/10.1080/02626667.2019.1620507.

[10] Borga M, Comiti F, Ruin I, Marra F (2019) Forensic analysis of flash flood response. Wiley Interdisciplinary Reviews: Water 6(2):e1338. https://doi.org/10.1002/wat2.1338.

[11] Borga M, Vezzani C, Dalla Fontana G (2005) Regional rainfall depth–duration–frequency equations for an alpine region. Natural Hazards 36(1):221–235. https://doi.org/10.1007/s11069-004-4550-y.

[12] Breugem AJ, Wesseling JG, Oostindie K, Ritsema CJ (2020) Meteorological aspects of heavy precipitation in relation to floods–an overview. Earth-Science Reviews 204:103171. https://doi.org/10.1016/j.earscirev.2020.103171.

[13] Buzzi A, Tartaglione N, Malguzzi P (1998) Numerical simulations of the 1994 Piedmont flood: Role of orography and moist processes. Monthly Weather Review 126(9):2369–2383. https://doi.org/10.1175/1520-0493(1998)126<2369:NSOTPF>2.0.CO;2.

[14] Cipolla G, Francipane A, Noto L (2020) Classification of extreme rainfall for a Mediterranean region by means of atmospheric circulation patterns and reanalysis data. Water Resources Management 34(10):3219–3235. https://doi.org/10.1007/s11269-020-02609-1.

[15] Correa-Sánchez N, Dallan E, Marra F, Fosser G, Borga M (2025) Orographic control on bias and uncertainty in extreme sub-daily precipitation simulations from a convection-permitting ensemble. Journal of Hydrology 659:133324. https://doi.org/10.1016/j.jhydrol.2025.133324.

[16] Dallan E, Borga M, Zaramella M, Marra F (2022) Enhanced summer convection explains observed trends in extreme subdaily precipitation in the Eastern Italian Alps. Geophysical Research Letters 49(5):e2021GL096727. https://doi.org/10.1029/2021GL096727.

[17] Dallan E, Marra F, Fosser G, Marani M, Formetta G, Schär C, Borga M (2023) How well does a convection-permitting regional climate model represent the reverse orographic effect of extreme hourly precipitation?. Hydrology and Earth System Sciences 27(5):1133–1149. https://doi.org/10.5194/hess-27-1133-2023.

[18] Dallan E, Borga M, Fosser G, Canale A, Roghani B, Marani M, Marra F (2024) A method to assess and explain changes in sub-daily precipitation return levels from convection-permitting simulations. Water Resources Research 60(5):e2023WR035969. https://doi.org/10.1029/2023WR035969.

[19] Davolio S, Della Fera S, Laviola S, Miglietta MM, Levizzani V (2020) Heavy precipitation over Italy from the Mediterranean storm “Vaia” in October 2018: Assessing the role of an atmospheric river. Monthly Weather Review 148(9):3571–3588. https://doi.org/10.1175/MWR-D-20-0021.1.

[20] Destro E, Amponsah W, Nikolopoulos EI, Marchi L, Marra F, Zoccatelli D, Borga M (2018) Coupled prediction of flash flood response and debris flow occurrence: Application on an alpine extreme flood event. Journal of Hydrology 558:225–237. https://doi.org/10.1016/j.jhydrol.2018.01.021.

[21] D'Odorico P, Fagherazzi S, Rigon R (2005) Potential for landsliding: Dependence on hyetograph characteristics. Journal of Geophysical Research: Earth Surface 110(F1). https://doi.org/10.1029/2004JF000127.

[22] Estermann R, Rajczak J, Velasquez P, Lorenz R, Schär C (2025) Projections of heavy precipitation characteristics over the greater Alpine region using a kilometer–scale climate model ensemble. Journal of Geophysical Research: Atmospheres 130(2):e2024JD040901. https://doi.org/10.1029/2024JD040901.

[23] Feloni EG, Baltas EA, Nastos PT, Matsangouras IT (2019) Implementation and evaluation of a convective/stratiform precipitation scheme in Attica region, Greece. Atmospheric Research 220:109–119. https://doi.org/10.1016/j.atmosres.2019.01.011.

[24] Fischer S, Schumann AH (2024) Temporal changes in the frequency of flood types and their impact on flood statistics. Journal of Hydrology X 22:100171. https://doi.org/10.1016/j.hydroa.2024.100171.

[25] Fischer S, Schumann AH (2021) Regionalisation of flood frequencies based on flood type-specific mixture distributions. Journal of Hydrology X 13:100107. https://doi.org/10.1016/j.hydroa.2021.100107.

[26] Fischer S, Schumann A, Bühler P (2019) Timescale-based flood typing to estimate temporal changes in flood frequencies. Hydrological Sciences Journal 64(15):1867–1892. https://doi.org/10.1080/02626667.2019.1679376.

[27] Frei C, Schär C (1998) A precipitation climatology of the Alps from high-resolution rain-gauge observations. International Journal of Climatology: A Journal of the Royal Meteorological Society 18(8):873–900. https://doi.org/10.1002/(SICI)1097-0088(19980630)18:8%3C873::AID-JOC255%3E3.0.CO;2-9.

[28] Grazzini F, Craig GC, Keil C, Antolini G, Pavan V (2020) Extreme precipitation events over northern Italy. Part I: A systematic classification with machine-learning techniques. Quarterly Journal of the Royal Meteorological Society 146(726):69–85. https://doi.org/10.1002/qj.3635.

[29] Grolemund G, Wickham H (2011) Dates and times made easy with lubridate. Journal of Statistical Software 40(3):1–25. https://doi.org/10.18637/jss.v040.i03.

[30] Gustafsson N, Janjić T, Schraff C, Leuenberger D, Weissmann M, Reich H, Brousseau P, Montmerle T, Wattrelot E, Bučánek A, et al. (2018) Survey of data assimilation methods for convective-scale numerical weather prediction at operational centres. Quarterly Journal of the Royal Meteorological Society 144(713):218–1256. https://doi.org/10.1002/qj.3179.

[31] Hastie T, Tibshirani R, Friedman J (2009) The Elements of Statistical Learning: Data Mining, Inference and Prediction, second edition. Springer, New York. https://doi.org/10.1007/978-0-387-84858-7.

[32] Herrera RV, Blenkinsop S, Guerreiro SB, Fowler HJ (2023) The creation and climatology of a large independent rainfall event database for Great Britain. International Journal of Climatology 43(13):6020–6037. https://doi.org/10.1002/joc.8187.

[33] Hijmans R (2025) raster: Geographic Data Analysis and Modeling. R package version 3.6-31. https://CRAN.R-project.org/package=raster.
[34] Hollister JW (2023) elevatr: Access Elevation Data from Various APIs. R package version 0.99.0. https://CRAN.R-project.org/package=elevatr.
[35] Hopke PK, Kaufman L (1990) The use of sampling to cluster large data sets. Chemometrics and Intelligent Laboratory Systems 8(2):195–204. https://doi.org/10.1016/0169-7439(90)80135-S.
[36] Isotta FA, Frei C, Weilguni V, Percec Tadic M, Lassegues P, Rudolf B, Pavan V, Cacciamani C, Antolini G, Ratto SM, et al. (2014) The climate of daily precipitation in the Alps: Development and analysis of a high-resolution grid dataset from pan-Alpine rain-gauge data. International Journal of Climatology 34(5):1657–1675. https://doi.org/10.1002/joc.3794.
[37] James G, Witten D, Hastie T, Tibshirani R (2013) An Introduction to Statistical Learning. Springer, New York. https://doi.org/10.1007/978-1-4614-7138-7.
[38] Kaczmarska J, Isham V, Onof C (2014) Point process models for fine-resolution rainfall. Hydrological Sciences Journal 59(11):1972–1991. https://doi.org/10.1080/02626667.2014.925558.
[39] Kahraman A, Kendon EJ, Chan SC, Fowler HJ (2021) Quasi-stationary intense rainstorms spread across Europe under climate change. Geophysical Research Letters 48(13):e2020GL092361. https://doi.org/10.1029/2020GL092361.
[40] Kahraman A, Kendon EJ, Fowler HJ, Wilkinson JM (2022) Contrasting future lightning stories across Europe. Environmental Research Letters 17(11):114023. https://doi.org/10.1088/1748-9326/ac9b78.
[41] Kassambara A (2023) ggpubr: 'ggplot2' Based Publication Ready Plots. R package version 0.6.0. https://CRAN.R-project.org/package=ggpubr.
[42] Kaufman L, Rousseeuw PJ (1990) Finding Groups in Data: An Introduction to Cluster Analysis. Wiley, New York.
[43] Kendall MG (1975) Rank Correlation Methods, fourth edition. Charles Griffin, London.
[44] Laaha G, Laimighofer J, Özcelik NB, Fischer S (2025) Exploring process heterogeneity in environmental statistics: Examples and methodological advances. Austrian Journal of Statistics 54(3):124–149. https://doi.org/10.17713/ajs.v54i3.2101.
[45] Llasat MC, del Moral A, Cortès M, Rigo T (2021) Convective precipitation trends in the Spanish Mediterranean region. Atmospheric Research 257:105581. https://doi.org/10.1016/j.atmosres.2021.105581.
[46] Maechler M, Rousseeuw P, Struyf A, Hubert M, Hornik K (2023) cluster: Cluster Analysis Basics and Extensions. R package version 2.1.6. https://CRAN.R-project.org/package=cluster.
[47] Mann HB (1945) Non-parametric tests against trend. Econometrica 13:163–171. https://doi.org/10.2307/1907187.
[48] Maraun D, Shepherd TG, Widmann M, Zappa G, Walton D, Gutiérrez JM, Hagemann S, Richter I, Soares PMM, Hall A, Mearns LO (2017) Towards process-informed bias correction of climate change simulations. Nature Climate Change 7(11):764–773. https://doi.org/10.1038/nclimate3418.
[49] Markonis Y, Kumar R, Hanel M, Rakovec O, Máca P, AghaKouchak A (2021) The rise of compound warm-season droughts in Europe. Science Advances 7(6):eabb9668. https://doi.org/10.1126/sciadv.abb9668.

[50] Marra F, Nikolopoulos EI, Creutin JD, Borga M (2014) Radar rainfall estimation for the identification of debris-flow occurrence thresholds. Journal of Hydrology 519(Part B):1607–1619. https://doi.org/10.1016/j.jhydrol.2014.09.039.
[51] Marra F, Borga M, Morin E (2020) A unified framework for extreme subdaily precipitation frequency analyses based on ordinary events. Geophysical Research Letters 47(18):e2020GL090209. https://doi.org/10.1029/2020GL090209.
[52] Marra F, Armon M, Adam O, Zoccatelli D, Gazal O, Garfinkel CI, Rostkier-Edelstein D, Dayan U, Enzel Y, Morin E (2021) Toward narrowing uncertainty in future projections of local extreme precipitation. Geophysical Research Letters 48(5):e2020GL091823. https://doi.org/10.1029/2020GL091823.
[53] Marra F, Koukoula M, Canale A, Peleg N (2024) Predicting extreme sub-hourly precipitation intensification based on temperature shifts. Hydrology and Earth System Sciences 28(2):375–389. https://doi.org/10.5194/hess-28-375-2024.
[54] Massicotte P, South A (2023) rnaturalearth: World Map Data from Natural Earth. R package version 1.0.1. https://CRAN.R-project.org/package=rnaturalearth.
[55] Ménégoz M, Valla E, Jourdain NC, Blanchet J, Beaumet J, Wilhelm B, Gallée H, Fettweis X, Morin S, Anquetin S (2020) Contrasting seasonal changes in total and intense precipitation in the European Alps from 1903 to 2010. Hydrology and Earth System Sciences 24(11):5355–5377. https://doi.org/10.5194/hess-24-5355-2020.
[56] Merz B, Aerts J, Arnbjerg-Nielsen K, Baldi M, Becker A, Bichet A, Blöschl G, Bouwer LM, Brauer A, Cioffi F, et al. (2014) Floods and climate: Emerging perspectives for flood risk assessment and management. Natural Hazards and Earth System Sciences 14:1921–1942. https://doi.org/10.5194/nhess-14-1921-2014.
[57] Napoli A, Parodi A, von Hardenberg J, Pasquero C (2023) Altitudinal dependence of projected changes in occurrence of extreme events in the Great Alpine Region. International Journal of Climatology 43(12):5813–5829. https://doi.org/10.1002/joc.8222.
[58] Neuwirth E (2022) RColorBrewer: ColorBrewer Palettes. R package version 1.1-3. https://CRAN.R-project.org/package=RColorBrewer.
[59] Papacharalampous GA, Dallan E, Armon M, Saha J, Price C, Borga M, Marra F (2025) Precipitation-driven typology of storms in the Alps: Data (Version v1) [Dataset]. Zenodo. https://doi.org/10.5281/zenodo.16418115.
[60] Papadopoulos A, Chronis TG, Anagnostou EN (2005) Improving convective precipitation forecasting through assimilation of regional lightning measurements in a mesoscale model. Monthly Weather Review 133(7):1961–1977. https://doi.org/10.1175/MWR2957.1.
[61] Peleg N, Morin E (2014) Stochastic convective rain-field simulation using a high-resolution synoptically conditioned weather generator (HiReS-WG). Water Resources Research 50(3):2124–2139. https://doi.org/10.1002/2013WR014836.
[62] Peleg N, Koukoula M, Marra F (2025) A 2C warming can double the frequency of extreme summer downpours in the Alps. npj Climate and Atmospheric Science 8:216. https://doi.org/10.1038/s41612-025-01081-1.
[63] Pineda N, Tomeu R, Joan B, Xavier S (2007) Lightning and precipitation relationship in summer thunderstorms: Case studies in the North Western Mediterranean region. Atmospheric Research 85(2):159–170. https://doi.org/10.1016/j.atmosres.2006.12.004.

[64] R Core Team (2024) R: A language and environment for statistical computing. R Foundation for Statistical Computing, Vienna, Austria. https://www.r-project.org.
[65] Ribeiro B, Velazco S, Guidoni-Martins K, Tessarolo G, Jardim L (2024) bdc: Biodiversity Data Cleaning. R package version 1.1.5. https://CRAN.R-project.org/package=bdc.
[66] Rodger CJ, Werner S, Brundell JB, Lay EH, Thomson NR, Holzworth RH, Dowden RL (2006) Detection efficiency of the VLF world-wide lightning location network (WWLLN): Initial case study. Annales Geophysical 24(12):3197–3214. https://doi.org/10.5194/angeo-24-3197-2006.
[67] Rubel F, Brugger K, Haslinger K, Auer I (2017) The climate of the European Alps: Shift of very high resolution Köppen-Geiger climate zones 1800–2100. Meteorologische Zeitschrift 26(2):115-125. https://doi.org/10.1127/metz/2016/0816.
[68] Ruiz-Leo AM, Hernández E, Queralt S, Maqueda G (2013) Convective and stratiform precipitation trends in the Spanish Mediterranean coast. Atmospheric Research 119:46–55. https://doi.org/10.1016/j.atmosres.2011.07.019.
[69] Rulfová Z, Kyselỳ J (2013) Disaggregating convective and stratiform precipitation from station weather data. Atmospheric Research 134:100–115. https://doi.org/10.1016/j.atmosres.2013.07.015.
[70] Rulfová Z, Kyselý J (2014) Trends of convective and stratiform precipitation in the Czech Republic, 1982–2010. Advances in Meteorology 2014:647938. https://doi.org/10.1155/2014/647938.
[71] Soriano LR, De Pablo F, Díez EG (2001) Relationship between convective precipitation and cloud-to-ground lightning in the Iberian Peninsula. Monthly Weather Review 129(12):2998–3003. https://doi.org/10.1175/1520-0493(2001)129<2998:RBCPAC>2.0.CO;2.
[72] Sottile G, Francipane A, Adelfio G, Noto LV (2022) A PCA-based clustering algorithm for the identification of stratiform and convective precipitation at the event scale: An application to the sub-hourly precipitation of Sicily, Italy. Stochastic Environmental Research and Risk Assessment 36(8):2303–2317. https://doi.org/10.1007/s00477-021-02028-7.
[73] Spinu V, Grolemund G, Wickham H (2024) lubridate: Make Dealing with Dates a Little Easier. R package version 1.9.4. https://CRAN.R-project.org/package=lubridate.
[74] Stein L, Pianosi F, Woods R (2020) Event-based classification for global study of river flood generating processes. Hydrological Processes 34(7):1514–1529. https://doi.org/10.1002/hyp.13678.
[75] Tarasova L, Merz R, Kiss A, Basso S, Blöschl G, Merz B, Viglione A, Plötner S, Guse B, Schumann A, et al. (2019) Causative classification of river flood events. Wiley Interdisciplinary Reviews: Water 6(4):e1353. https://doi.org/10.1002/wat2.1353.
[76] Tarasova L, Basso S, Wendi D, Viglione A, Kumar R, Merz R (2020) A process-based framework to characterize and classify runoff events: The event typology of Germany. Water Resources Research 56(5):e2019WR026951. https://doi.org/10.1029/2019WR026951.
[77] Tremblay A (2005) The stratiform and convective components of surface precipitation. Journal of the Atmospheric Sciences 62(5):1513–1528. https://doi.org/10.1175/JAS3411.1.

[78] Treppiedi D, Cipolla G, Noto LV (2023) Convective precipitation over a Mediterranean area: From identification to trend analysis starting from high-resolution rain gauges data. International Journal of Climatology 43(1):293–313. https://doi.org/10.1002/joc.7758.

[79] Tseng CY, Wang LP, Onof C (2025) Modelling convective cell life cycles with a copula-based approach. Hydrology and Earth System Sciences 29(1):1–25. https://doi.org/10.5194/hess-29-1-2025.

[80] Virts KS, Wallace JM, Hutchins ML, Holzworth RH (2013) Highlights of a new ground-based, hourly global lightning climatology. Bulletin of the American Meteorological Society 94(9):1381–1391. https://doi.org/10.1175/bams-d-12-00082.1.

[81] Warnes G, Bolker B, Bonebakker L, Gentleman R, Huber W, Liaw A, Lumley T, Maechler M, Magnusson A, Moeller S, et al. (2024) gplots: Various R Programming Tools for Plotting Data. R package version 3.2.0. https://CRAN.R-project.org/package=gplots.

[82] Weisse AK, Bois P (2001) Topographic effects on statistical characteristics of heavy rainfall and mapping in the French Alps. Journal of Applied Meteorology 40(4):720–740. https://doi.org/10.1175/1520-0450(2001)040<0720:TEOSCO>2.0.CO;2.

[83] Wickham H (2023) tidyverse: Easily Install and Load the 'Tidyverse'. R package version 2.0.0. https://CRAN.R-project.org/package=tidyverse.

[84] Wickham H, Averick M, Bryan J, Chang W, McGowan LD, François R, Grolemund G, Hayes A, Henry L, Hester J, et al. (2019) Welcome to the tidyverse. Journal of Open Source Software 4(43):1686. https://doi.org/10.21105/joss.01686.

[85] Wickham H, Bryan J (2023) readxl: Read Excel Files. R package version 1.4.3. https://CRAN.R-project.org/package=readxl.

[86] Wickham H, Hester J, Chang W, Bryan J (2022) devtools: Tools to Make Developing R Packages Easier. R package version 2.4.5. https://CRAN.R-project.org/package=devtools.

[87] Wickham H, François R, Henry L, Müller K, Vaughan D (2023a) dplyr: A Grammar of Data Manipulation. R package version 1.1.4. https://CRAN.R-project.org/package=dplyr.

[88] Wickham H, Pedersen T, Seidel D (2023b) scales: Scale Functions for Visualization. R package version 1.3.0. https://CRAN.R-project.org/package=scales.

[89] Wilke C (2024) ggridges: Ridgeline Plots in 'ggplot2'. R package version 0.5.6. https://CRAN.R-project.org/package=ggridges.

[90] Xie Y (2014) knitr: A Comprehensive Tool for Reproducible Research in R. In: Stodden V, Leisch F, Peng RD (Eds) Implementing Reproducible Computational Research. Chapman and Hall/CRC.

[91] Xie Y (2015) Dynamic Documents with R and knitr, second edition. Chapman and Hall/CRC.

[92] Xie Y (2024) knitr: A General-Purpose Package for Dynamic Report Generation in R. R package version 1.49. https://CRAN.R-project.org/package=knitr.

[93] Xie Y, Allaire JJ, Grolemund G (2018) R Markdown: The Definitive Guide. Chapman and Hall/CRC. ISBN 9781138359338. https://bookdown.org/yihui/rmarkdown.

[94] Xie Y, Dervieux C, Riederer E (2020) R Markdown Cookbook. Chapman and Hall/CRC. ISBN 9780367563837. https://bookdown.org/yihui/rmarkdown-cookbook.

[95] Zhou K, Zheng Y, Li B, Dong W, Zhang X (2019) Forecasting different types of convective weather: A deep learning approach. Journal of Meteorological Research 33:797–809. https://doi.org/10.1007/s13351-019-8162-6.